JOURNAL OF SYNCHROTRON RADIATION
ISSN 1600-5775

A setup for synchrotron-radiation-induced total reflection X-ray fluorescence and X-ray absorption near-edge structure recently commissioned at BESSY II BAMline

U. Fittschen,[a]* A. Guilherme,[b] S. Böttger,[c] D. Rosenberg,[c] M. Menzel,[d] W. Jansen,[c] M. Busker,[c] Z. P. Gotlib,[a] M. Radtke,[b] H. Riesemeier,[b] P. Wobrauschek[e] and C. Streli[e]

[a]Chemistry Department, Washington State University, Pullman, WA 99164, USA, [b]BAM, Bundesanstalt für Materialforschung und -prüfung, 12489 Berlin, Germany, [c]Chemistry and Chemistry Education Department, Europa-Universität Flensburg, 24943 Flensburg, Germany, [d]Chemistry Department, University of Hamburg, 20146 Hamburg, Germany, and [e]Atominstitut, Vienna University of Technology, Vienna 1020, Austria. *Correspondence e-mail: ursula.fittschen@wsu.edu

Received 1 October 2015
Accepted 1 February 2016

Edited by P. A. Pianetta, SLAC National Accelerator Laboratory, USA

Keywords: TXRF; TXRF-XANES; sample changer; BAMline; Re-XANES.

An automatic sample changer chamber for total reflection X-ray fluorescence (TXRF) and X-ray absorption near-edge structure (XANES) analysis in TXRF geometry was successfully set up at the BAMline at BESSY II. TXRF and TXRF-XANES are valuable tools for elemental determination and speciation, especially where sample amounts are limited (<1 mg) and concentrations are low (ng ml^{-1} to µg ml^{-1}). TXRF requires a well defined geometry regarding the reflecting surface of a sample carrier and the synchrotron beam. The newly installed chamber allows for reliable sample positioning, remote sample changing and evacuation of the fluorescence beam path. The chamber was successfully used showing accurate determination of elemental amounts in the certified reference material NIST water 1640. Low limits of detection of less than 100 fg absolute (10 pg ml^{-1}) for Ni were found. TXRF-XANES on different Re species was applied. An unknown species of Re was found to be Re in the +7 oxidation state.

1. Introduction

1.1. TXRF and TXRF-XANES

Synchrotron-radiation-based total reflection X-ray fluorescence analysis (SR-TXRF) is an analytical technique allowing for quasi non-destructive, simultaneous multi-element analysis of minute amounts of a sample (<1 mg). Coupled with X-ray absorption near-edge structure spectroscopy (XANES), this technique now provides information about the electronic structure of the elements of interest. Early work on XAS in total reflection geometry was performed in the late 1980s and early 1990s (Heald *et al.*, 1986; Dartyge *et al.*, 1986; Asakura *et al.*, 1993; Kawai *et al.*, 1993). The advantages of using SR-TXRF and SR-TXRF/XANES lie in the fact that limits of absolute detection are in the low femtogram (fg µL^{-1}) and picogram (pg µL^{-1}) regions, respectively, whereas, using laboratory TXRF setups, typical lower limits of detection fall in the picogram range (Klockenkämper & von Bohlen, 2015). TXRF-XANES requires tunable radiation by maintaining relatively high primary beam flux densities and is, therefore, usually solely pursued at synchrotron facilities.

Synchrotron-based TXRF has been proven very useful for different applications. One is the determination of elements in

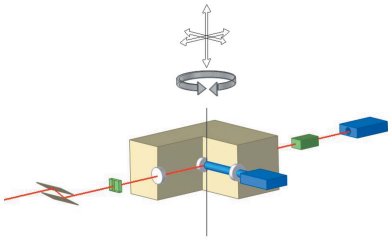

atmospheric aerosols to monitor atmospheric events (short time scale, 1 h sampling time), an application that requires the analysis of minute amounts of sample (sub-µg). Several groups have used this technique to study elemental concentration in aerosol particulate matter (Fittschen *et al.*, 2008; Osán *et al.*, 2010).

Speciation of elements in p.p.m. concentration in these minute amounts of sample is challenging for conventional setups but achievable in TXRF-XANES geometry (Fittschen *et al.*, 2008; Meirer *et al.*, 2007). Meirer *et al.* report a limit of detection of 32 p.p.b. for speciation of As in the xylem sap of plants. The results of the study indicate that cucumber plants reduce As^{V} to As^{III} (Meirer *et al.*, 2007).

Other potential applications are the speciation of trace concentrations of hazardous elements in pore water (water held within a soil or rock, in gaps between particles) or valuable elements from sediments. The oxidation state is critical for the mobility of elements such as Tc and actinides found in sediments of sites contaminated by the nuclear industry, or valuable elements such as Re which have a complex redox chemistry. Identifying their oxidation state under a certain environmental condition allows one to understand and predict the dynamic behaviour of the respective element. This will eventually advance remediation of contaminated sites and exploitation of valuable elements such as noble and rare-earth metals.

1.2. Advantage of a sample changer

TXRF spectrometry is sensitive to the deviation of the angle of incidence and the solid angle captured by the detector. However, fine tuning of the angle of incidence and assuring low angle deviation over the irradiated surface area is time-consuming and limits the output achievable within the time frame of normal user beam time. Accordingly, equipment that ensures optimal and constant measurement conditions increases output and accuracy of measured data. A few examples for beamlines more frequently used for TXRF analysis are: PTB at BESSY II, BAMline at BESSY II and beamline L at Doris III. Only beamline L was equipped with an automated sample chamber for SR-TXRF until the Doris synchrotron ring was shut down in 2012. This chamber was modified to fit the BAMline and figures-of-merit were determined.

2. Sample chamber and periphery

The general design of the sample chamber is described by Streli *et al.* (2006). The setup allows users to record SR-TXRF and SR-TXRF-XANES spectra with high reproducibility on 30 mm-diameter quartz sample holders. The sample holder has been designed to allow synchrotron light to interact with the sample at a grazing angle of below 0.1° with the detector setup in the polarization plane of the incoming radiation. The setup consists of an Al chamber with a fitting for a vacuum line, two Kapton windows (8 µm) and a vacuum feedthrough fitting for an energy-dispersive XRF detector. The first Kapton window is the entrance for the primary beam into the chamber and the second Kapton window is the exit for both the reflected beam and the primary beam passing over the reflector without reflection. The core of the chamber is the sample positioning unit in front of the detector, consisting of three metal balls and a pressure spring sample holder that keeps the sample carriers in a defined plane relative to the primary beam and the detector. A Ta wedge on the side of the incoming beam ensures a minimum of scattering from the reflector rim. The chamber is designed for vacuum operation, an ideal feature for reducing remaining scatter from air. It also removes the Ar *K* line arising from the Ar content of ambient air and reduces absorption allowing for low detection limits in light-element detection.

The chamber was installed at the BAMline (Bundesanstalt für Materialforschung und -prüfung) of the Berlin electron storage ring (BESSY II). Details of the BAMline design are given by Riesemeier *et al.* (2005). This experimental station is a high-energy beamline for XRF measurements at BESSY II at the Helmholtz-Zentrum Berlin. At this beamline the primary radiation source is a 7 T wavelength shifter (Wiedemann, 2010; Borovikov *et al.*, 1998; Görner *et al.*, 2001).

The chamber was mounted on an XYZ stage and goniometer table (Huber, Rimsting, Germany). The angle between the reflector plane and the incoming beam was adjusted by the goniometer. A silicon drift detector (SDD) (XFlash 5010; Bruker AXS, Berlin, Germany) with a 30 mm^2 active area was used to collect XRF spectra. Fig. 1 shows a sketch of the general setup with the chamber; Fig. 2 shows an image of the sample positioning unit, two of three steel balls forming the reference plane and the Ta wedge; Fig. 3 shows the setup at the BAMline.

3. Data acquisition and application

A double multilayer monochromator was used for the analysis of Ni samples and analysis of NIST water 1640. A beam size of 1.5 mm × 1.5 mm (width × height) was used and an acquisition time of 1000 s was chosen for the purpose.

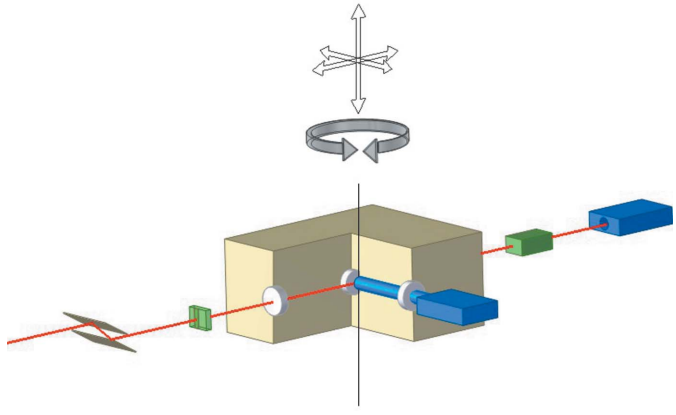

Figure 1
Sketch of the sample chamber showing all major components and its positioning at the BAMline.

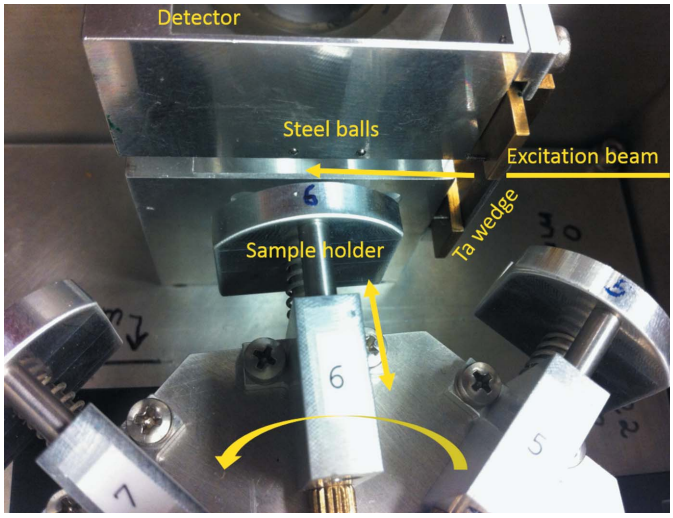

Figure 2
Inside the chamber showing the sample holder, the steel balls forming the reference plane as well as the Ta wedge.

For the Re XANES acquisition, the energy of the X-ray beam was tuned by a double-crystal Si (111) monochromator. A beam size of 4 mm × 4 mm was used and the acquisition time was 100 s per energy.

The software *Athena* from the *IFEFFIT* suite was used to process the XANES data (Ravel & Newville, 2005; Newville, 2001). All measurements were performed in air.

3.1. Limits of detection (LOD) for Ni

TXRF is a very common analytical tool in the Si-wafer industry. An established procedure in Si-wafer TXRF is the determination of the LOD for low concentrations of Ni contamination. In this respect, LOD for Ni were determined in this work. Specimens containing Ni in concentrations of 100 pg and 10 pg were prepared from pipetting 10 µL of diluted Ni single-element standard solutions (Merck Millipore, Darmstadt, Germany) and ultra-pure water (Omnitrace®, Merck Millipore, Darmstadt, Germany) on a 30 mm-diameter quartz reflector. The LOD were determined according to the following equation,

$$\mathrm{LOD} = \frac{3\,Ci\,(N_\mathrm{B})^{1/2}}{N_i}, \qquad (1)$$

where Ci is the concentration of Ni, N_B is the background count and N_i is the net count of Ni $K\alpha$.

For the 10 pg Ni specimens and 1000 s measurement time, a LOD value of 60 fg was found. This current value is around ten times more than our earlier findings (Streli *et al.*, 2006), but is explained by the fact that at the time of the experiments presented here the detector had a smaller active area and had not yet been incorporated into the beamline electronics, and the measurements were performed under air atmosphere. The LODs are considerably lower compared with a conventional laboratory setup. A comparison is given in Table 1. As the detection limit is an extrapolated value based on statistical considerations, it is to be expected that the 10 pg sample is not detectable using the TXRF laboratory setup.

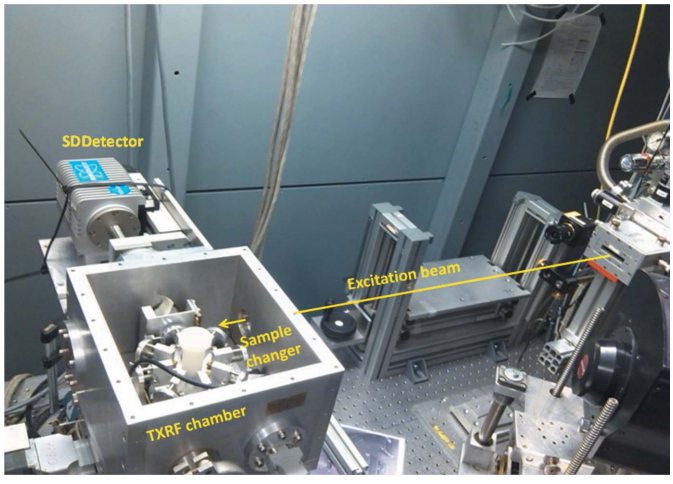

Figure 3
View into the open chamber showing the sample changer.

Table 1
LODs for Ni determined using the newly installed setup at the BAMline and a laboratory TXRF setup (calculated for 1000 s lifetime).

Amount of Ni (pg)	LODs Sy-TXRF (pg)	LOD conventional TXRF (pg) low-power TXRF†
10	0.06	<detection limit
100	0.07	8

† *A Low Power Mo Tube TXRF Spectrometer with Electrically Cooled Silicon Drift Detector* (Wobrauschek *et al.*, 2011).

3.2. Accuracy of water analysis

Trace elemental determination in minute amounts of aqueous samples (<1 ml) is a general application area for TXRF, *e.g.* analysis of pore water, Xylem sap from plants, *etc*.

In order to determine the accuracy of the analysis of small amounts of an aqueous sample, 10 µL samples of NIST water 1640 were prepared on a quartz reflector and analyzed for 100 s. The spectra were fitted using *PyMCA* (Solé *et al.*, 2007); Cu was used as internal standard and a fundamental parameter approach was used to determine the concentration of all detectable elements. Fig. 4 shows the spectrum acquired at the BAMline and fitted using *PyMCA*. Table 2 shows the detected and certified elements and their concentrations as certified and determined at the BAMline. All elements above the detection limits were found to deviate by at most <10% from the certified concentrations. However, the Ni, Cr and Ba concentrations deviated by 20–30%.

3.3. Re L_3-edge XANES

Elemental speciation of metal ions in low concentrations is maybe the most valuable and also the most challenging application of SR-TXRF; valuable because of its unique capabilities for trace element speciation offering p.p.b. LOD, while ensuring minimum interference with the sample and, therefore, reducing the risk of alteration, and challenging

Table 2
Elemental concentrations certified for NIST water 1640 and determined at the BAMline with SR-TXRF.

Element	Line	Certified amount (μg L^{-1})	Determined amount (μg L^{-1})	Deviation (%)
K	*Kα*	994.00	912.44	8.20
Ca	*Kα*	7045.00	6872.37	2.45
V	*Kα*	12.99	12.77	1.66
Cr	*Kα*	38.60	26.84	30.47
Mn	*Kα*	121.50	118.91	2.13
Fe	*Kα*	34.30	34.05	0.73
Co	*Kα*	20.28	18.13	10.62
Ni	*Kα*	27.40	32.69	19.30
Cu(IS)	*Kα*	85.20	85.20	0.00
Zn	*Kα*	53.20	56.56	6.31
Ba	*Lα*	148.00	118.18	20.15

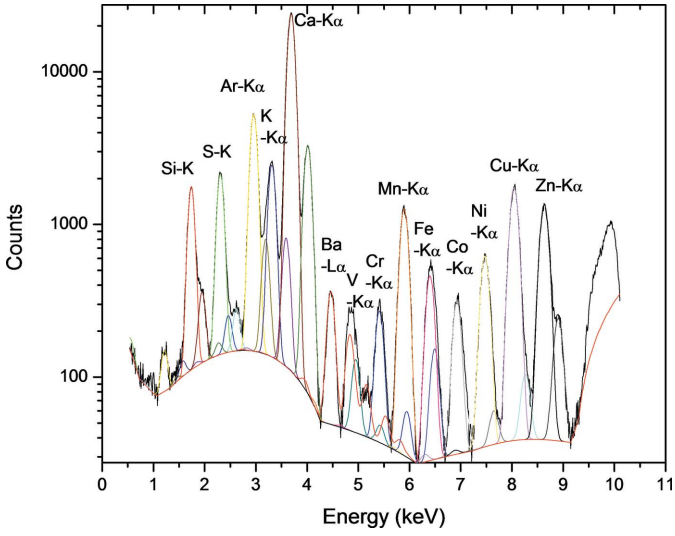

Figure 4
SR-TXRF spectrum of the NIST water 1640 specimen fitted using *PyMCA*, acquired at the BAMline.

because self-absorption effects well known in fluorescence yield XANES increase for small angles as applied in TXRF. However, a number of publications addressed this problem in the past and made modelling and experimental solutions available to solve this problem (Lühl *et al.*, 2012; Meirer *et al.*, 2008, 2009; Menzel *et al.*, 2013).

Here we focused on the speciation of Re. Re has a complex redox chemistry, is of interest as a catalyst and, therefore, stands as an example for a valuable element. Re is also a non-radioactive substitute for Tc, which is a critically hazardous element regarding nuclear contaminated sites. Fluorescence yield XANES usually requires spectra at the L_3-edge using the *Lα* line. The allowed transition from the 2*p* state to the 5*d* state is dominant and leads to the distinct white line. For the 5*d* states located at the central atom, the energy of the ground and the excited states changes during oxidation, though the shift at the L_3-edge is quite small. The height of the white line is a measure of the density of excited states and accordingly of the oxidation state as well. Tougerti *et al.* (2012) found a shift

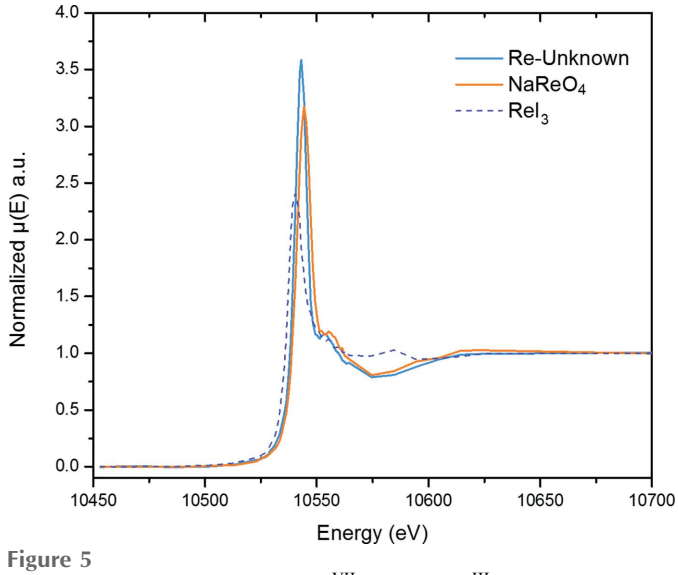

Figure 5
XANES spectra of $NaReO_4$ (Re^{VII}), ReI_3 (Re^{III}) and an unknown compound.

of ∼1 eV per formal oxidation state for Re oxides at the L_3-edge.

Here, an unknown aqueous Re solution and two known Re compounds with defined oxidation states $NaReO_4$ (Re^{VII}) and ReI_3 (Re^{III}) were prepared from suspensions to ensure a minimum of alteration of the specimen. The procedure was described by Fittschen *et al.* (2008). The concentration of Re in the compounds was 5 ng and 6 ng, respectively, determined using a laboratory TXRF instrument (Picofox S2, Bruker, Berlin, Germany).

The TXRF-XANES study on the reference compounds showed an edge shift of 3 eV between $NaReO_4$ and ReI_3, which is shown in Fig. 5. Compared with the results of Tougerti *et al.* (2012), this corresponds to a change in oxidation state from +7 to +4; however, ReI_3 is formally in a +3 oxidation state. It is likely that a part of the ReI_3 was oxidized by oxygen in ambient air to Re +7, which is a quite stable state. The difference in the heights of the white line of both compounds is also apparent. Following normalization to the post edge, the white line for ReI_3 rises to 1.50 units above the post-edge line and to 2.20 units for $NaReO_4$, which is explained by the higher density of excited states in Re +7 (see paragraph above).

The speciation of 1 ng Re in an unknown Re complex revealed a good correlation to the XANES spectrum of $NaReO_4$. The amount was determined prior to the TXRF-XANES measurements using a laboratory TXRF instrument (Picofox S2, Bruker, Berlin, Germany).

Fig. 5 shows the normalized XANES spectra for the three compounds. Fig. 6 shows the derivatives of the XANES spectra. The edge shifts of the unknown and $NaReO_4$ were not significantly different. It can be assumed that both compounds have a formal oxidation state of +7. However, the small shift indicates a difference in the chemical species of the unknown. The height of the white line of the unknown was 2.50 units. This is different from the height found for $NaReO_4$ and is caused by self-absorption effects due to differences in the total

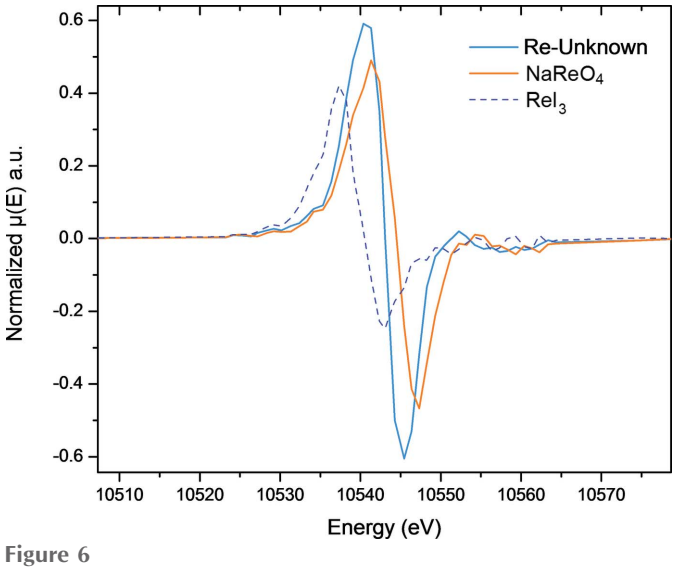

Figure 6
Derivative of the edge regions of the XANES spectra shown in Fig. 5.

amount of Re in the respective specimen. The unknown with the lowest absolute mass of 1 ng Re shows a minimum in self-absorption effects.

4. Conclusion

The TXRF setup at the BAMline at BESSY II is now available to all users and is currently the only available synchrotron-based total reflection X-ray spectrometer of its kind. It is part of a growing TXRF community that has recently been reviewed by Klockenkämper & von Bohlen (2014).

Acknowledgements

We acknowledge the Helmholtz-Zentrum Berlin for provision of synchrotron radiation beam time at the BAMline of BESSY II. CS and PW thankfully acknowledge the financial support from HZB. The research leading to these results has received funding from the European Community's Seventh Framework Programme (FP7/2007–2013) under grant agreement No. 312284. The authors thank Katharina Peikert and Dr Paul Benny for providing Re materials. The presented work has received funding from the Austrian Science Fund (FWF), project No. P23832-N20.

References

Asakura, K., Shirai, M. & Iwasawa, Y. (1993). *Catal. Lett.* **20**, 117–124.
Borovikov, V. M., Craft, B., Fedurin, M. G., Jurba, V., Khlestov, V., Kulipanov, G. N., Li, O., Mezentsev, N. A., Saile, V. & Shkaruba, V. A. (1998). *J. Synchrotron Rad.* **5**, 440–442.
Dartyge, E., Fontaine, A., Tourillon, G., Cortes, R. & Jucha, A. (1986). *Phys. Lett. A*, **113**, 384–388.
Fittschen, U. E. A., Meirer, F., Streli, C., Wobrauschek, P., Thiele, J., Falkenberg, G. & Pepponi, G. (2008). *Spectrochim Acta B*, **63**, 1489–1495.
Görner, W., Hentschel, M. P., Müller, B. R., Riesemeier, H., Krumrey, M., Ulm, G., Diete, W., Klein, U. & Frahm, R. (2001). *Nucl. Instrum. Methods Phys. Res. A*, **467–468**, 703–706.
Heald, S. M., Tranquada, J. M. & Chen, H. J. (1986). *J. Phys.* **47**(C-8), 293–298.
Kawai, J., Hayakawa, S., Kitajima, Y., Suzuki, S., Maeda, K., Urai, T., Adachi, H., Takami, M. & Gohshi, Y. (1993). *Proc. Jpn Acad. Ser. B*, **69**, 179–184.
Klockenkämper, R. & von Bohlen, A. (2014). *Spectrochim Acta B*, **99**, 133–137.
Klockenkamper, R. & von Bohlen, A. (2015). *Total-Reflection X-ray Fluorescence Analysis and Related Methods*, 2nd ed. New York: Wiley.
Lühl, L., Mantouvalou, I., Malzer, W., Schaumann, I., Vogt, C., Hahn, O. & Kanngiesser, B. (2012). *Anal. Chem.* **84**, 1907–1914.
Meirer, F., Pepponi, G., Streli, C., Wobrauschek, P., Kregsamer, P., Zoeger, N. & Falkenberg, G. (2008). *Spectrochim Acta B*, **63**, 1496–1502.
Meirer, F., Pepponi, G., Streli, C., Wobrauschek, P., Mihucz, V. G., Záray, G., Czech, V., Broekaert, J. A. C., Fittschen, U. E. A. & Falkenberg, G. (2007). *X-ray Spectrom.* **36**, 408–412.
Meirer, F., Pepponi, G., Streli, C., Wobrauschek, P. & Zoeger, N. (2009). *J. Appl. Phys.* **105**, 074906.
Menzel, M., Schlifke, A., Falk, M., Janek, J., Fröba, M. & Fittschen, U. E. A. (2013). *Spectrochim Acta B*, **85**, 62–70.
Newville, M. (2001). *J. Synchrotron Rad.* **8**, 322–324.
Osán, J., Meirer, F., Groma, V., Török, S., Ingerle, D., Streli, C. & Pepponi, G. (2010). *Spectrochim Acta B*, **65**, 1008–1013.
Ravel, B. & Newville, M. (2005). *J. Synchrotron Rad.* **12**, 537–541.
Riesemeier, H., Ecker, K., Görner, W., Müller, B. R., Radtke, M. & Krumrey, M. (2005). *X-ray Spectrom.* **34**, 160–163.
Solé, V., Papillon, E., Cotte, M., Walter, P. & Susini, J. (2007). *Spectrochim Acta B*, **62**, 63–68.
Streli, C., Pepponi, G., Wobrauschek, P., Jokubonis, C., Falkenberg, G., Záray, G., Broekaert, J., Fittschen, U. & Peschel, B. (2006). *Spectrochim Acta B*, **61**, 1129–1134.
Tougerti, A., Cristol, S., Berrier, E., Briois, V., La Fontaine, C., Villain, F. & Joly, Y. (2012). *Phys. Rev. B*, **85**, 125136.
Wiedemann, H. (2010). *Synchrotron Radiation.* Berlin/Heidelberg: Springer.
Wobrauschek, P., Felling, C., Prost, J. & Streli, C. (2011). *XRF Newsl.* **22**(2), 16.